Electronic Supplementary Material (ESI) for Journal of Materials Chemistry A.

Supporting Information

Controlling pore size and pore functionality in sp^2- conjugated microporous materials by precursor chemistry and salt templating

Sol Youk[1], Jan P. Hofmann[2], Bolortuya Badamdorj[1], Antje Völkel[1], Markus Antonietti[1], Martin Oschatz[1,3,]*

[1] Max Planck Institute of Colloids and Interfaces, Colloid Chemistry, Research Campus Golm, Am Muhlenberg 1, D-14476 Potsdam, Germany

[2] Laboratory for Inorganic Materials and Catalysis, Department of Chemical Engineering and Chemistry, Eindhoven University of Technology, P.O. Box 513, 5600 MB, Eindhoven, The Netherlands

[3] Institute of Chemistry, University of Potsdam, Karl-Liebknecht-Str. 24-25, D-14476 Potsdam, Germany

*Corresponding author. Email: martin.oschatz@mpikg.mpg.de

Supplementary Tables

Table S1. EA summary of samples with and without pre-condensation.

	N-content (wt.%)	C-content (wt.%)	H-content (wt.%)	C/N	SSA_{BET} $[m^2\ g^{-1}]$
NOC-550	18.0	54.6	3.1	3.5	532
NOC-550 without pre-condensation	11.3	57.0	3.5	5.1	457
NOC-550 Without pre-condensation and melamine	9.3	57.8	3.0	6.2	290

Table S2. XPS data summary for atomic and weight percentage (rounded to two significant digits) of elements in the samples.

	C-content (at.%) (wt.%)	N-content (at.%) (wt.%)	O-content (at.%) (wt.%)	Zn-content (at.%) (wt.%)	Cl-content (at.%) (wt.%)	Others (at.%)	C/N (at. ratio)
NOC-350	58 (53)	29 (31)	11 (14)	0.1 (0.4)	0.9 (2.3)	-	2.0
NOC-550	74 (69)	20 (21)	6.0 (7.5)	-	0.6 (1.8)	0.1	3.8
NOC-750	78 (73)	15 (17)	5.0 (6.2)	0.2 (1.1)	0.9 (2.6)	-	5.1
NOC-950	87 (83)	5.1 (5.6)	6.3 (8.0)	0.1 (0.3)	0.7 (1.9)	0.5	17.1
NOC-350-550	74 (69)	20 (22)	6.4 (8.0)	0.2 (1.0)	0.1 (0.3)	-	3.7
NOC-550-750	82 (76)	13 (14)	3.7 (4.6)	0.8 (4.0)	0.5 (1.5)	-	6.2
NOC-550-950	93 (91)	4.6 (5.3)	2.8 (3.7)	0.1 (0.3)	-	-	20.1

Supplementary Figures

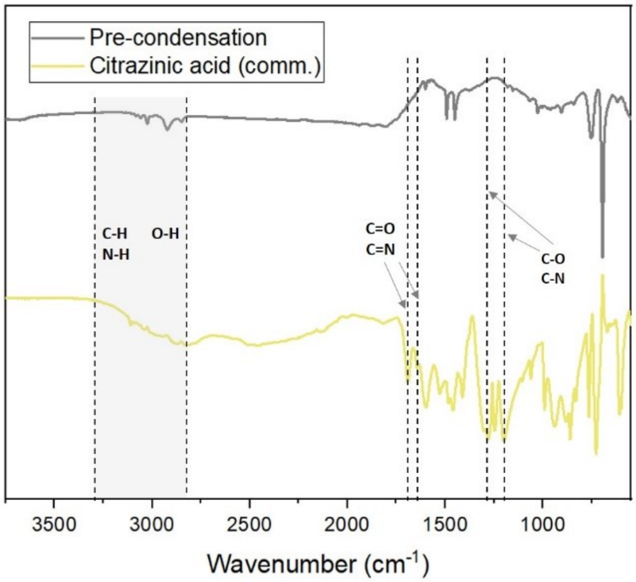

Figure S1. FT-IR spectra of commercial citrazinic acid and the product after pre-condensation.

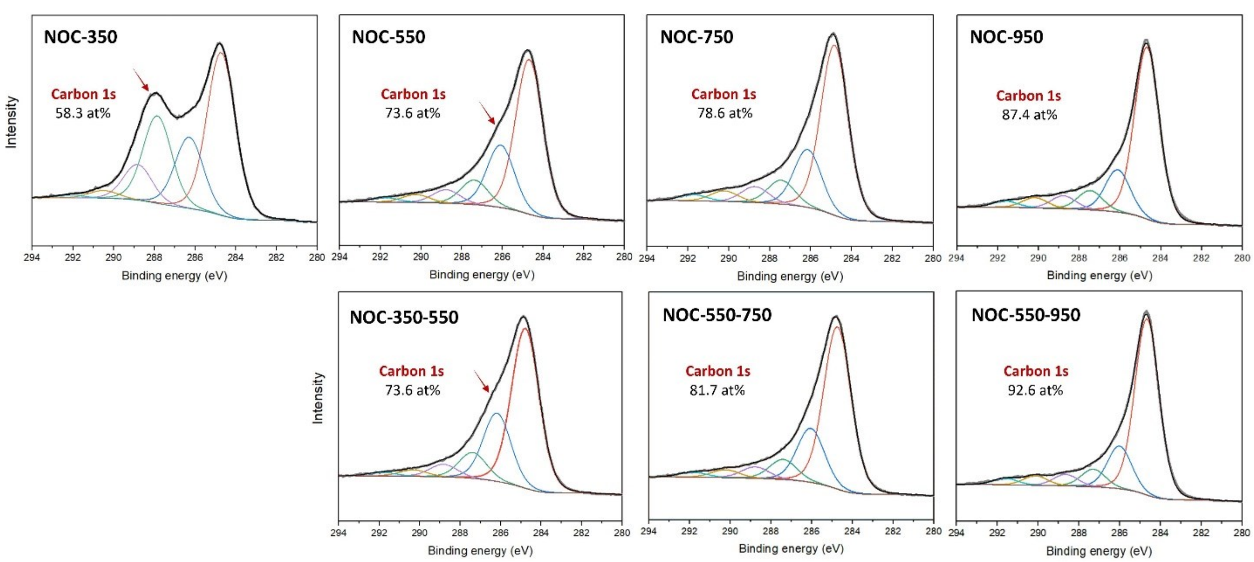

Figure S2. High-resolution C1s XPS spectra and corresponding fitting curves of NOC-Xs and NOC-X-Ys.

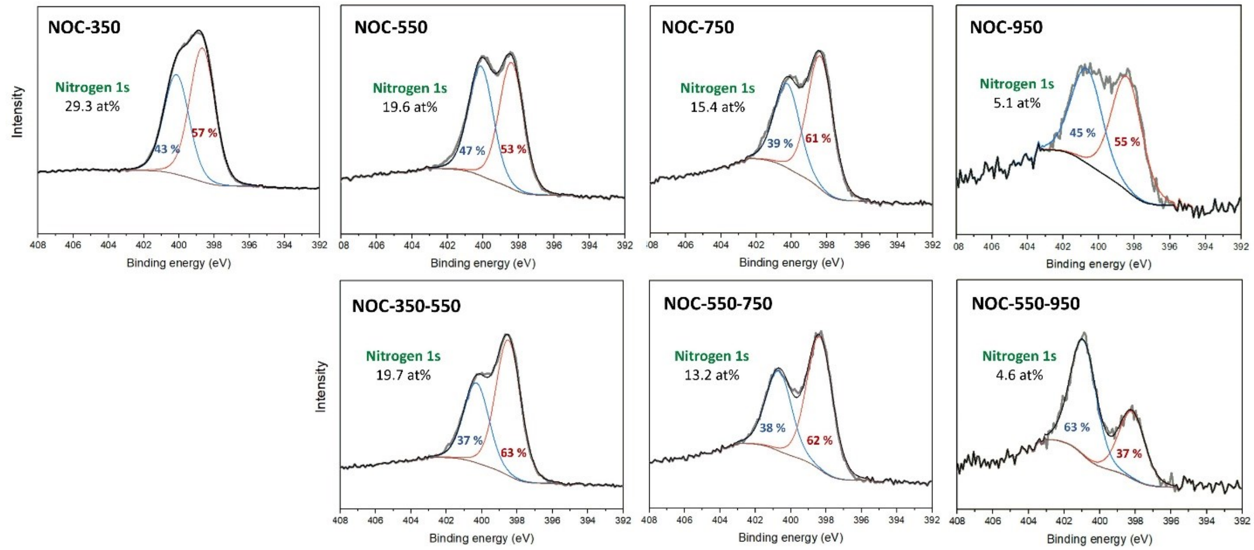

Figure S3. High-resolution N1s XPS spectra and corresponding fitted curves of NOC-Xs and NOC-X-Ys.

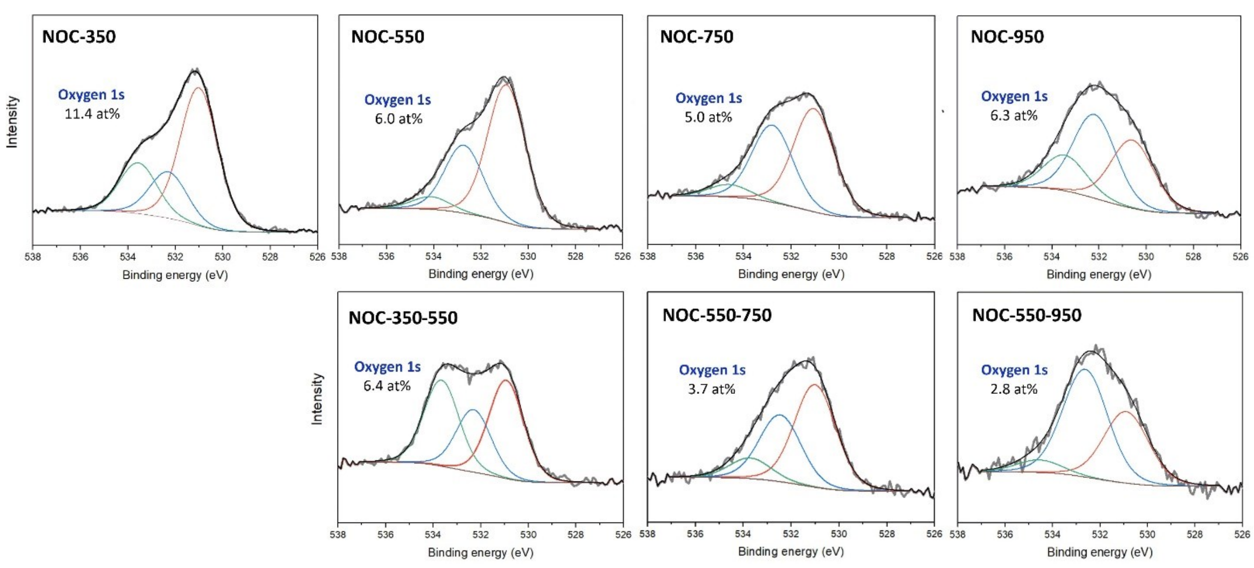

Figure S4. High-resolution O1s XPS spectra and corresponding fitted curves of NOC-Xs and NOC-X-Ys.

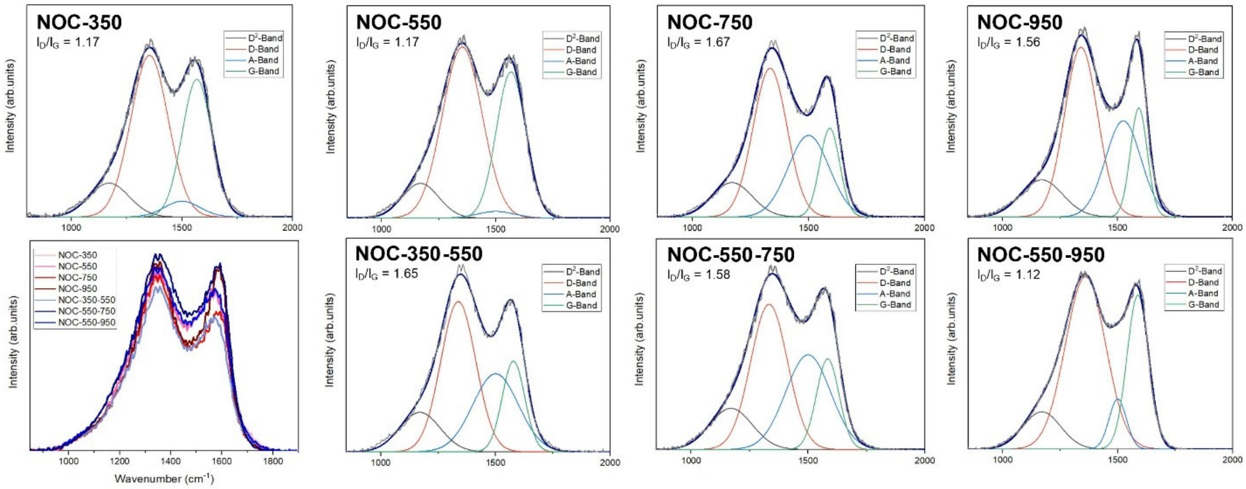

Figure S5. Fitted Raman spectra of NOC-Xs and NOC-X-Ys.

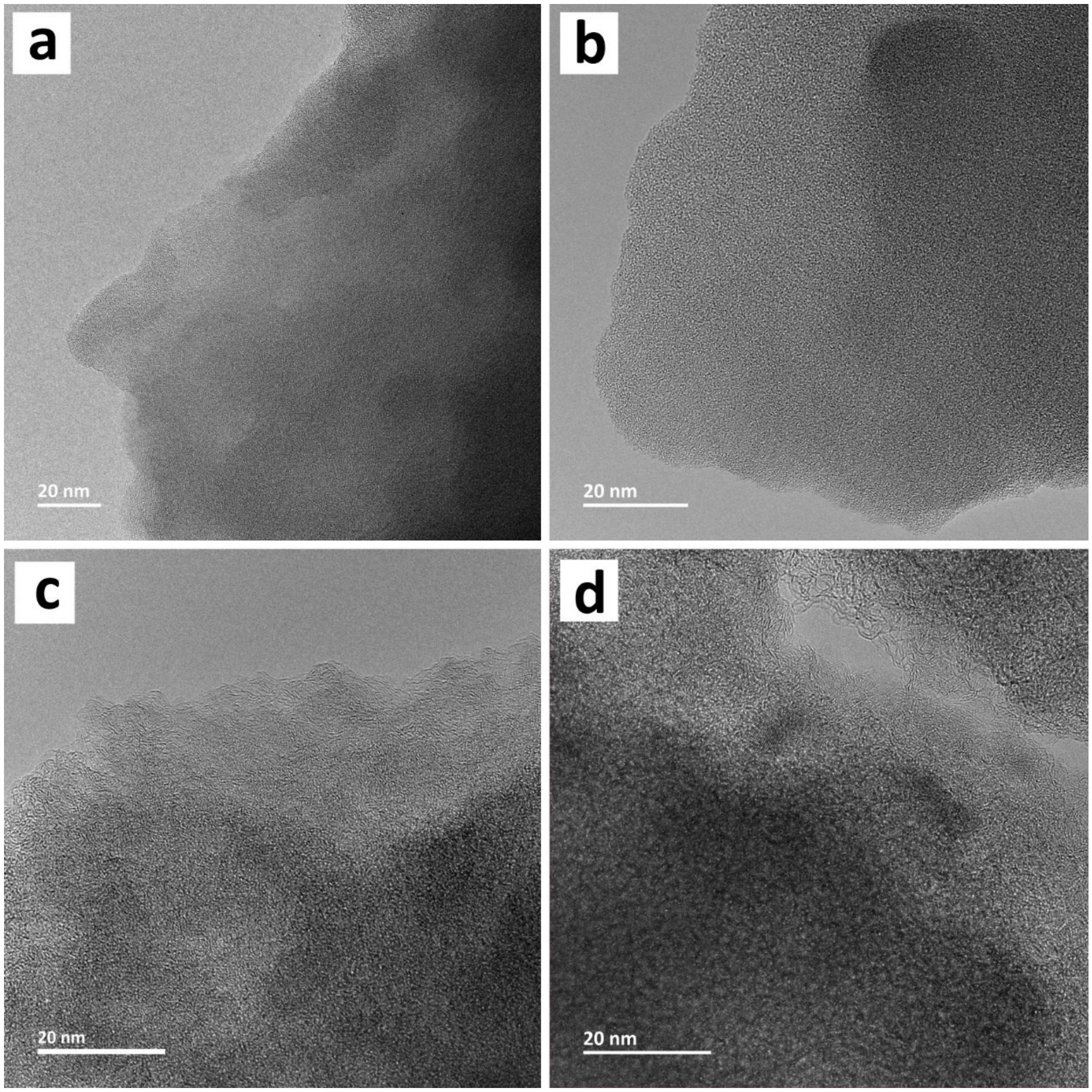

Figure S6. High-resolution transmission electron microscopy (HRTEM) images of (a) NOC-350, (b) NOC-550, (c) NOC-750, and (d) NOC-950.

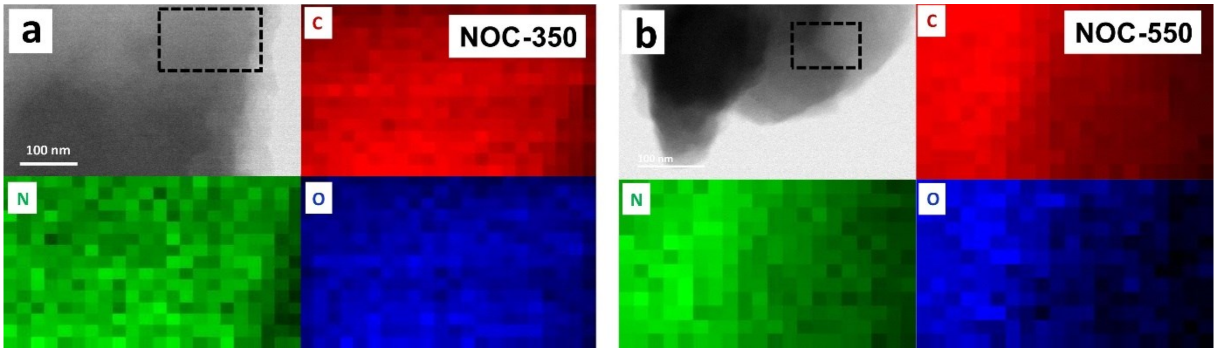

Figure S7. EDX elemental mapping of C (red), N (greed), and O (blue) of (a) NOC-350 and (b) NOC-550.

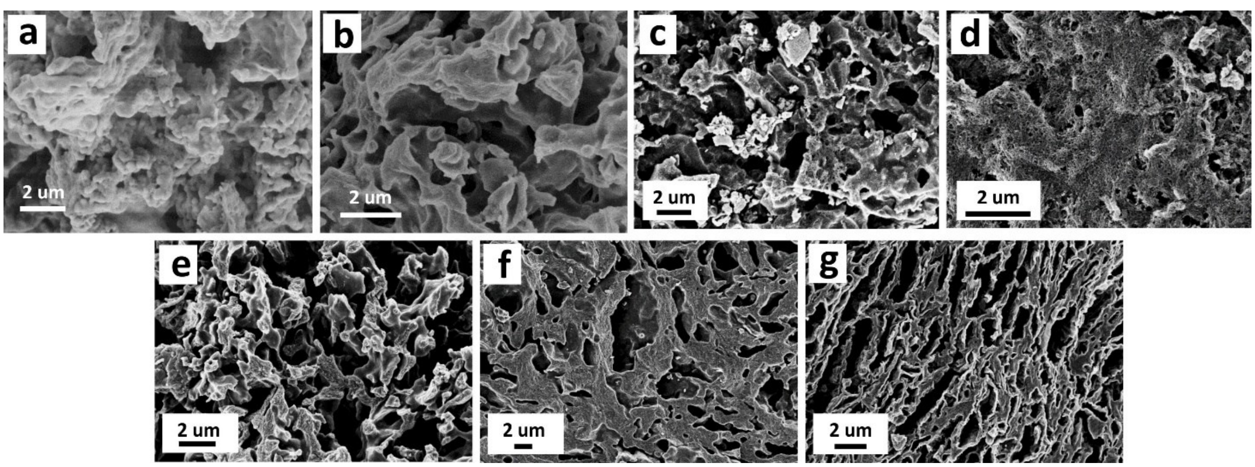

Figure S8. Scanning electron microscopy (SEM) images of (a) NOC-350, (b) NOC-550, (c) NOC-750, (d) NOC-950, (e) NOC-350-550, (f) NOC-550-750, and (g) NOC-550-950.

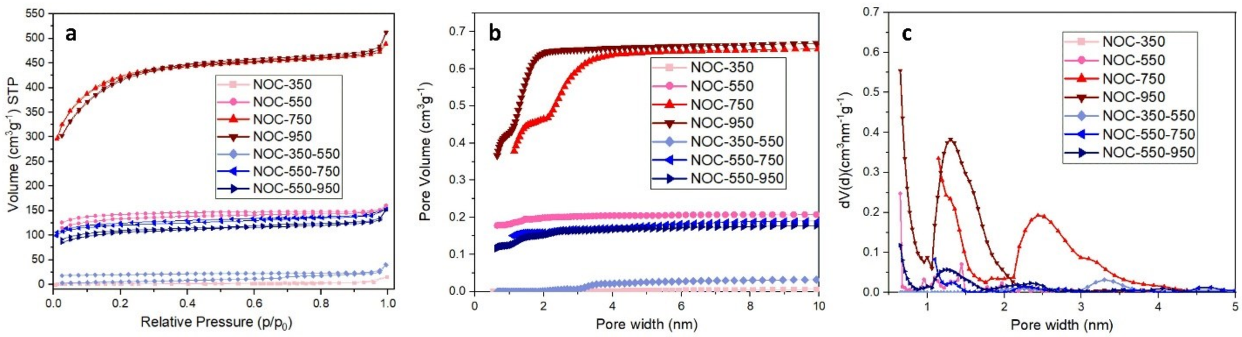

Figure S9. (a) N_2 physisorption isotherms (77 K), (b) corresponding cumulative pore volume distribution, and (c) differential pore size distribution calculated with QSDFT (N_2 on carbons with cylindrical/sphere pores at 77 K) of NOC-Xs and NOC-X-Ys.

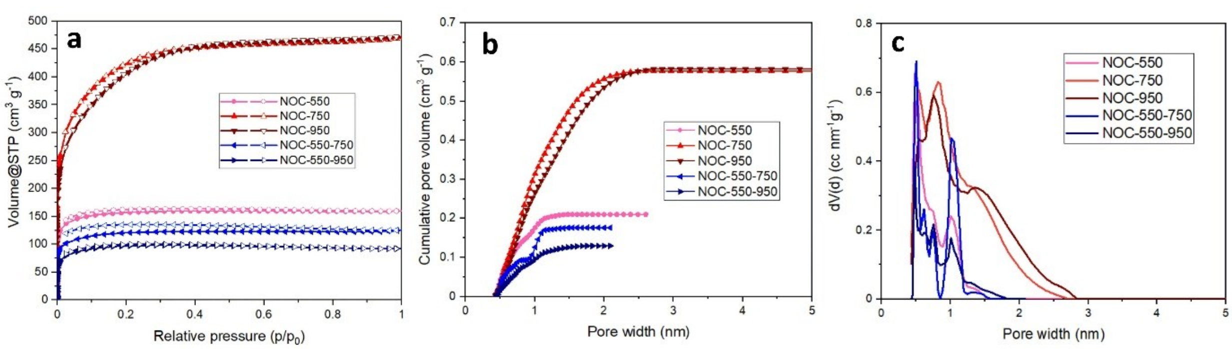

Figure S10. (a) Argon physisorption isotherms (87 K, filled and open symbols represent adsorption and desorption branches, respectively), (b) corresponding cumulative pore volume distribution, and (c) differential pore size distribution calculated with QSDFT equilibrium model (argon on carbons with slit pores at 87 K) of NOC-Xs and NOC-X-Ys.

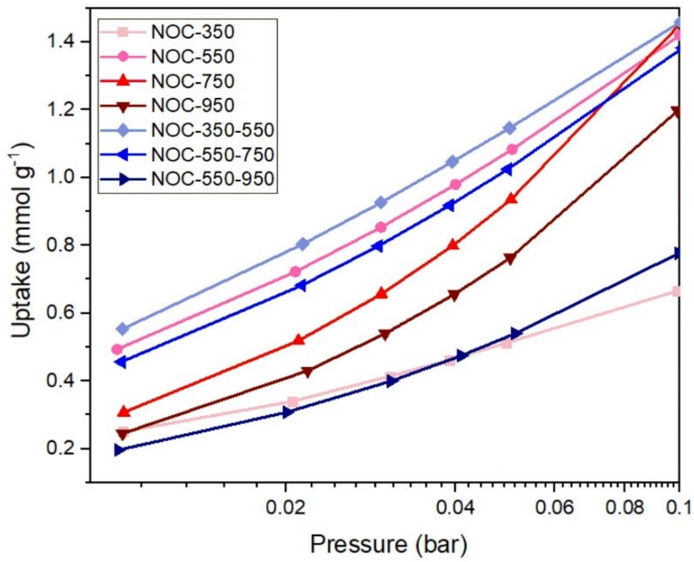

Figure S11. Logarithmic plots of CO_2 isotherms (273 K) in the low pressure range.

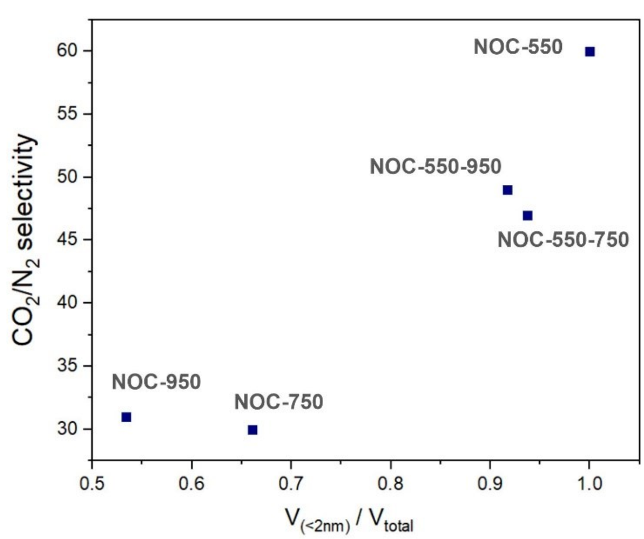

Figure S12. Relation between the CO_2/N_2 selectivity at 273 K and the ratio of micropore volume to total pore volume from Ar physisorption.

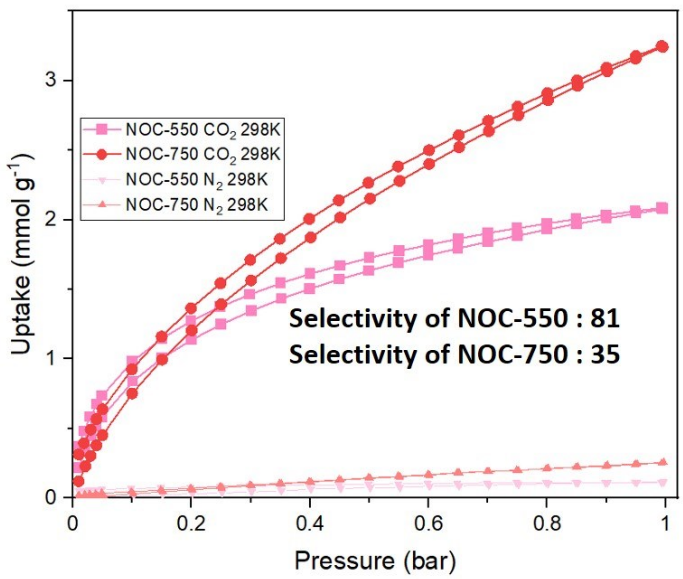

Figure S13. (a) CO_2 and N_2 physisorption isotherms of NOC-550 and NOC-750 measured at 298 K.

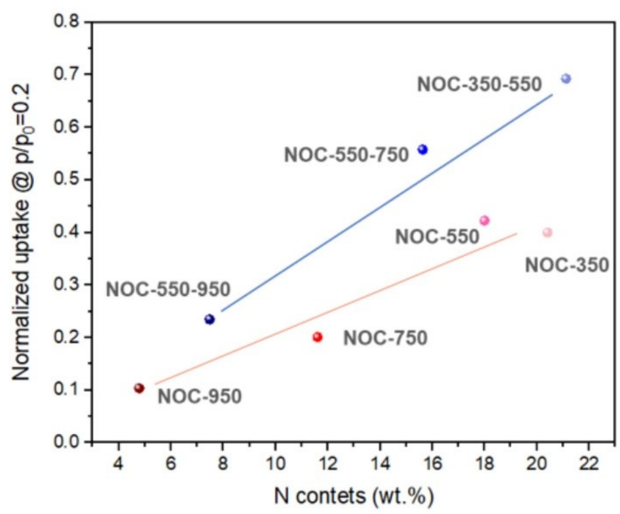

Figure S14. The normalized uptake at relative pressure $p/p_0 = 0.2$ as a function of the N content of NOC-Xs and NOC-X-Ys from EA.